Supporting Information

Boronate Affinity Imprinted Inverse Opal Particles for Multiple Label-Free Bioassays

Huan Wang, Qionghua Xu, Luoran Shang, Jie Wang, Yuanjin Zhao,* Fei Rong,* Zhongze Gu*

State Key Laboratory of Bioelectronics, School of Biological Science and Medical Engineering, Southeast University, Nanjing 210096, China;

Laboratory of Environment and Biosafety, Research Institute of Southeast University in Suzhou, Suzhou 215123, China

Email: yjzhao@seu.edu.cn; gu@seu.edu.cn

Experimental

Materials

Polyethylene glycol (PEG) 200 (average molecular weight, 190.0-210.0), Poly (ethylene glycol) diacrylate (PEGDA, average molecular weight, 700), horseradish peroxidase, ribonuclease A, ribonuclease B, holo-transferrin human, and 2-hydroxy-2-methylpropiophenone (HMPP) photoinitiator were obtained from Sigma-Aldrich (St. Louis, MO, USA). Hydrofluoric acid and one-component TMB substrate were bought from Aladdin Industrial Corporation (Shanghai, China). Ethanol and n-hexane were purchased from Sinopharm Chemical Reagent (Shanghai, China). 4-Vinylbenzeneboronic (4-VPBA) was purchased from Alfa Aesar China Ltd (Heysham, Lancs). Artificial urine were bought from InnoReagents, (Huzhou, China). SiO2 nanoparticles in different sizes were obtained from Nanjing Dongjian Biological Technology Co., Ltd. All solutions were prepared with DI water.

Other reagents were analytical grade or higher and all the reagents were used as received.

Fabrication of template silica colloidal crystal beads (SCCBs)

The SCCBs were generated by the droplet template method. The silicon oil and aqueous suspension were injected into the microfluidic device through different channels. The concentration of the aqueous suspension was adjusted to 20 wt% before used. The flow rates of the oil and water phase were 4mL/h and 0.5mL/h, respectively. When the device was running, the aqueous phase was cut into droplets by the oil phase when they met in the confluence of the microfluidic channel. The droplets were collected in silicon oil with high viscosity. After that, the droplets container was transferred to oven at 75°C so that the silica nanoparticles can self-assemble into ordered lattices during the evaporation of water. After overnight solidification, the SCCBs were washed with n-hexane gently and thoroughly to remove the residual silicon oil. At last, the SCCBs were calcined at 800°C for 4h to enhance their mechanical strength. The reflection spectra of the SCCBs were measured by the metalloscope (OLYMPUS BX51) with a fiber optic spectrometer (Ocean Optics, QE65000), the photographs of the SCCBs were taken by the metalloscope (OLYMPUS BX51) with a CCD camera (Media Cybernetics EvolutionMP 5.0) and the scanning electron microscopy (SEM, Hitachi, S-300N) was used to characterize the microstructures of the SCCBs.

Investigation of the best composition for MIP inverse opal particles

A series of pregel solution were prepared with the PEGDA in 5%, 15%, 25%, 35% (v/v), PEG in 0%, 20%, 40%, 60% (v/v), HMPP in 1% (v/v) and H_2O for the rest. The mixed solution was stirred about 10min. The inverse opal particles were polymerized with the pregel and the structures were replicated from the voids of the template SCCBs. To ensure the pregel solution could fill the void entirely, the SCCBs were treated with piranha solution (oil of vitriol: hydrogen peroxide=7:3, v/v) overnight. Then, the SCCBs were immersed in the pregel about 2h and followed by treating with UV curing. The polymerized gel with SCCBs was soaked with buffer solution for

30min in succession. As the gel can swell in the buffer while the SCCBs showed little change, the SCCBs can peel off the gel easily. Finally, the inverse opal particles were obtained after the removal of the silica and templates by immersed in hydrofluoric acid (4%, v/v) for 2h. The resulted particles were photographed by a metalloscope and shown in **Fig. S2**.

Fabrication of MIP inverse opal particles

1mg VPBA and 2μL HMPP were dissolved in 40μL PEG 200 and mixed with 40μL Tris-HCl (pH=8.5). The mixed solution was stirred about 10min. Then 20μL stock solution of the templates (10mg/mL in water), 50μL PEGDA 700 and 48μL DI water were added to the mixture and stirred about 5min. The resulting solution was pregel. The next steps were the same mentioned above. For the fabrication of NIP, the stock solution of the templates was replaced with water in the same volume, while the other reagents and steps were treated in the same.

Target glycoprotein capture and detection

The reflection spectra of the as-prepared MIP and NIP inverse opal particles were measured in water before reaction. Then they were put in the solution of target glycoprotein in different concentration (0, 1ng/mL, 10ng/mL, 100ng/mL, 1μg/mL, 10μg/mL, 100μg/mL, and 1mg/mL) for 3h. After that, the inverse opal particles were washed gently in water thrice to remove the glycoprotein on the inverse opal particles because of adsorption. Finally, the reflection spectra of the inverse opal particles were measured and the change compared with the results before reaction and the shift were shown in **Fig.** 3, **Fig.** 4, **Fig.** S3 and **Fig.** S5. For demonstration of the multiplexing capabilities of the MIP inverse opal particles, the solution was replaced with the mixture of HRP and RNase B at 1mg/mL respectively and the other steps were in the same. When the TRF-imprinted MIP and NIP were used for detecting the TRF in artificial urine, the TRF was dispersed in artificial urine with different concentrations.

Measurement of adsorption isotherm

We investigated the binding capability of the HRP-imprinted MIP and NIP by the steady-state binding method. As the particles are too small for detecting, 0.2g SiO_2 nanoparticles were dissolved in H_2O for every centrifuge tube and centrifuged at 8000 rpm for 15 min, the supernatant was removed and colloidal crystals were assembled. After dried in constant temperature oven at 45°C for 2 days, the crystals were calcined at 800°C for 4h to enhance their mechanical strength. Then the crystals were immersed in 200μL HRP pregel about 2h and followed by treating with UV curing. The crystals with hydrogel were treated with hydrofluoric acid (4%, v/v) for 2 days. After washed by buffer solution, 600μL HRP in different concentrations were added into the centrifugal tubes with resulting hydrogels and shaken 12h. The amounts of HRP bound to the MIP or NIP were determined by measuring the residual HRP in the centrifugal tubes. The amount of residual HRP were measured by mixing 1μL supernatant diluted 10-fold with 100μL one-component TMB substrate and incubating for 10 min, adding 100μL H_2SO_4 (1M), and then detecting by UV absorbance at 450 nm. The hydrogels at the outside of the crystals were collected and dried by vacuum freeze dryer, and the weight were compared with hydrogel polymerized without nanoparticles to calculate the HRP in the crystals. When the hydrogels were used for HRP capture, the water in the hydrogels were considered to be a part of the volume of the HRP solution, the volume were estimated by comparing the weight of the hydrogels with the hydrogels prepared in the same and dried by vacuum freeze dryer. As the detection for the other glycoproteins required the use of HRP-conjugated antibodies, which led to large errors, the adsorption isotherms for the other glycoproteins are not reported. The results were shown in Fig. S4 and the imprinting factor and binding capacity can be calculated with the results.

Supporting Figures:

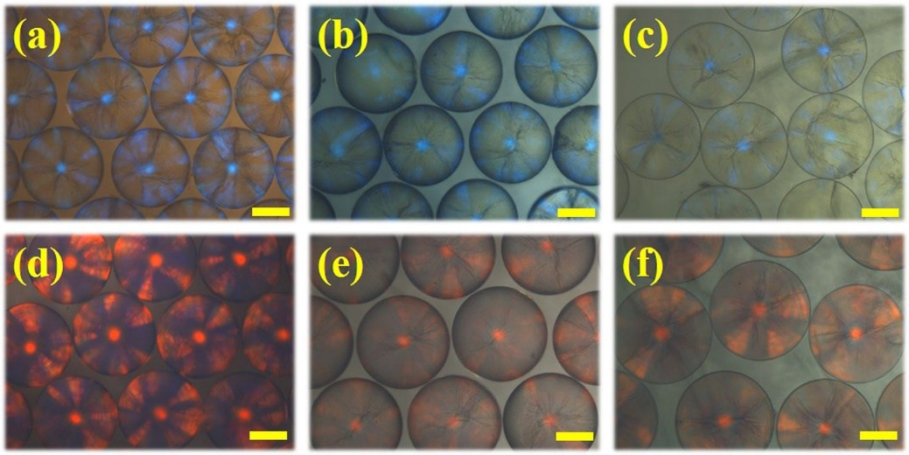

Fig. S1 Reflection microscope images of (a, d) the blue and red structural color SCCBs, (b, e) the corresponding MIP hydrogel hybrid SCCBs, and (c, f) the corresponding MIP inverse opal particles. Scale bars are 100μm.

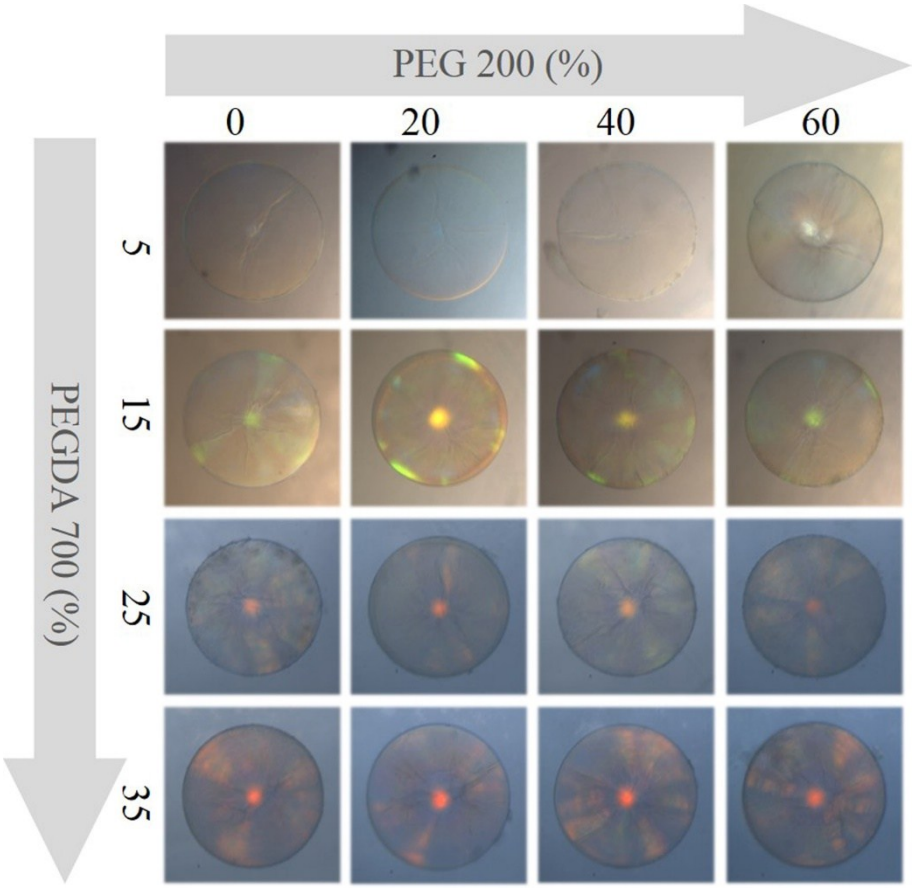

Fig. S2 Reflection microscope images of MIP inverse opal particles that composed of different concentrations of PEG hydrogels.

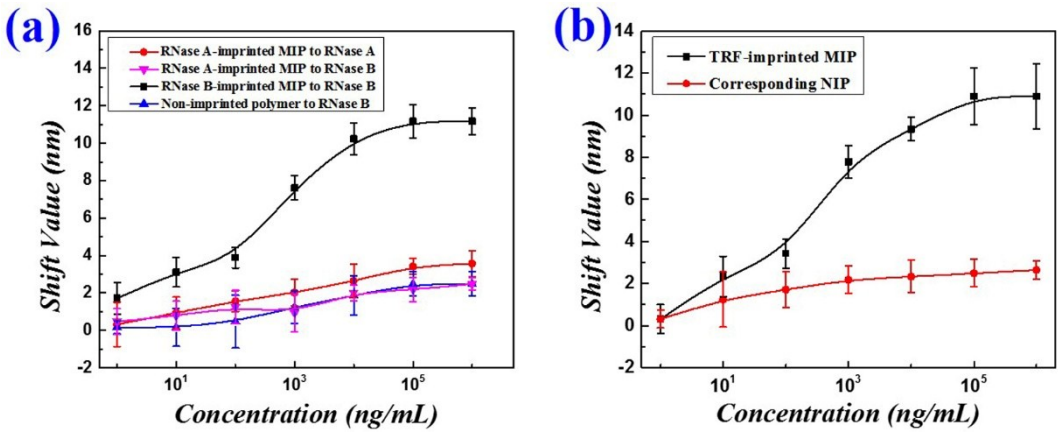

Fig. S3 (a) Bragg diffraction peak shift values of the RNase A-imprinted, RNase B-imprinted and non-imprinted inverse opal particles in different concentrations of the RNase B, and the RNase A-imprinted inverse opal particles in different concentrations of the RNase A. (b) Bragg diffraction peak shift values of the TRF-imprinted and non-imprinted inverse opal particles in different concentrations of the TRF. The RNase B MIP showed high selectivity to the RNase B due to the specific recognition of the boronic MIP to the glycoprotein molecules. However, the RNase A MIP was with low selectivity to the RNase A and RNase B. The number of replicates at any concentration was five. Error bars represent standard deviations.

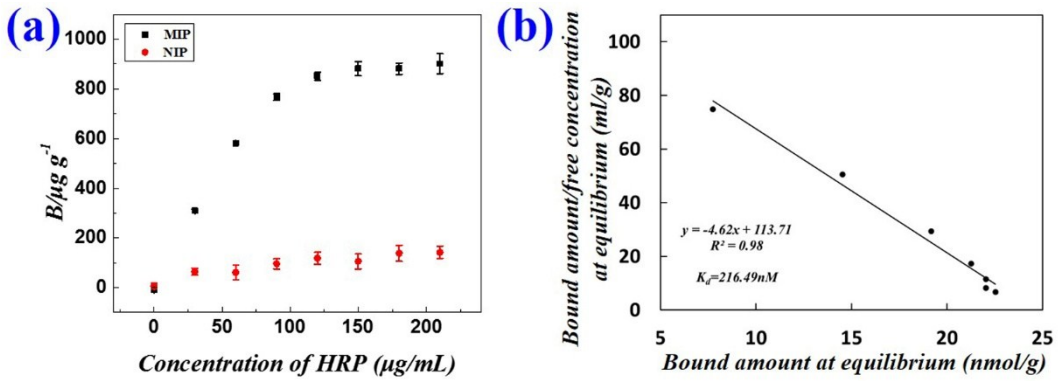

Fig. S4 (a) the binding isotherms of HRP-imprinted MIP and the corresponding NIP. (b) Scatchard analysis plot for the binding of the HRP to the MIP. The amount of the HRP bound to the MIP was plotted according to the Scatchard equation, and imprinted factor and binding capacity can be calculated from the diagram. The Scatchard equation was shown as below:

$$\frac{B}{F} = \frac{B_{max}}{K_d} - \frac{B}{K_d}$$

The B was the amount of the HRP bound to the MIP at equilibrium, F was the free concentration in solution at equilibrium, Bmax was the saturated adsorption capacity of the MIP, and Kd was dissociation constant. Plotting the B/F versus B, the dots presented a linear distribution. After fitting, the Kd and Bmax can be calculated from the slope and the intercept, respectively. The linear distribution of the dots indicated that there was only one kind of binding site formed in the MIP. It is worth noting that the calculated Kd and Bmax are only a rough estimation of the MIP, because only a portion of the surface and inner face of the MIP contributed to the apparent binding properties. The Kd of the MIP in the experiment may be slightly different from the actual value, and the experimental Bmax (24.62 nmol/g) is probably lower than the actual value.

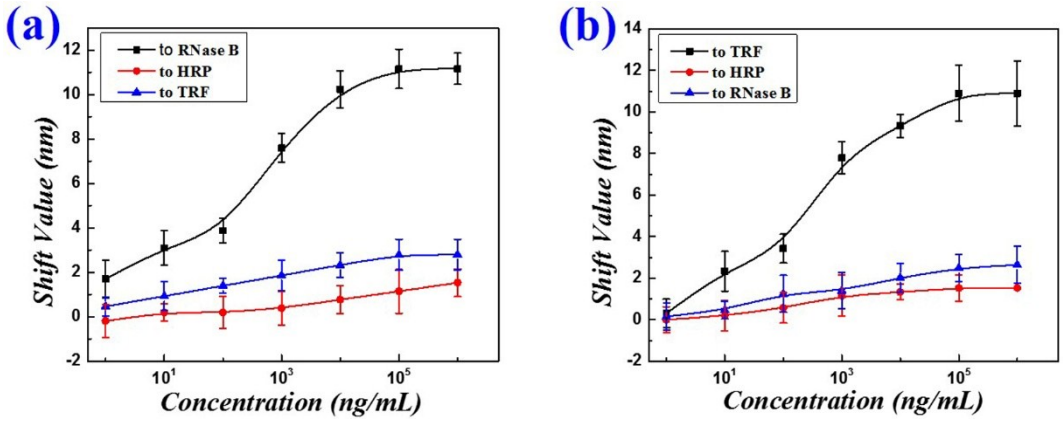

Fig. S5 Plot of the Bragg shifts for the (a) RNase B and (b) TRF imprinted inverse opal particles in response to solutions of HRP, RNase B, and TRF at different concentrations. The number of replicates at any concentration was five. Error bars represent standard deviations.

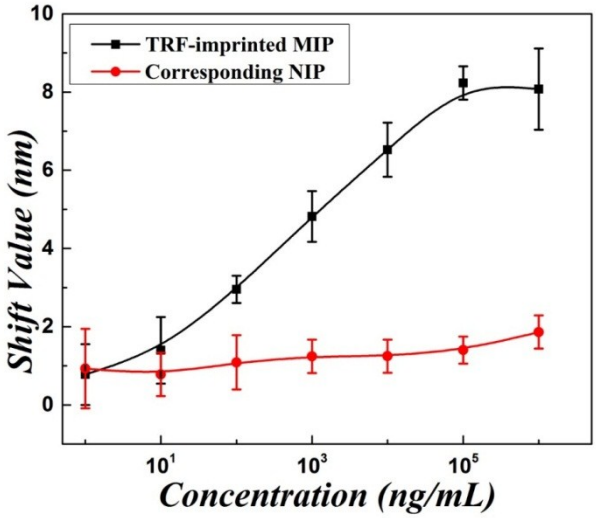

Fig. S6 Bragg diffraction peak shift values of the imprinted and non-imprinted inverse opal particles of TRF in artificial urine with different concentrations of TRF.